Microscopic mechanism of electric-field-induced superconductivity suppression in metallic thin films

Microscopic mechanism of electric-field-induced superconductivity suppression in metallic thin films

Alessio Zaccone [1], Giovanni Alberto Ummarino [2], Alessandro Braggio,[3] and Francesco Giazotto [3]
[1]*Department of Physics "A. Pontremoli," University of Milan, via Celoria 16, 20133 Milan, Italy*
[2]*Politecnico di Torino, Dipartimento di Scienza Applicata e Tecnologia, corso Duca degli Abruzzi 24, 10129 Torino, Italy*
[3]*NEST, Istituto Nanoscienze-CNR and Scuola Normale Superiore, I-56127 Pisa, Italy*

(Received 12 February 2025; revised 6 May 2025; accepted 9 May 2025; published 27 May 2025)

Supercurrent field-effect transistors made from thin metallic films are a promising option for next-generation high-performance computing platforms. Despite extensive research, there is still no complete quantitative microscopic explanation for how an external dc electric field suppresses superconductivity in thin films. This study aims to provide a quantitative description of superconductivity as a function of film thickness based on Eliashberg's theory. The calculation considers the electrostatics of the electric field, its realistic penetration depth in the film, and its effect on the Cooper pair, which is described as a standard *s*-wave bound state according to BCS theory. The estimation suggests that an external electric field of approximately 10^8 V/m is required to suppress superconductivity in films 10–30 nm thick, which aligns with experimental observations. Ultimately, the study offers "materials-by-design" guidelines for suppressing supercurrent when an external electric field is applied to the film surface. Furthermore, the proposed framework can be easily extended to investigate the same effects for ultrathin films.

DOI: 10.1103/PhysRevB.111.174528

I. INTRODUCTION

Supercurrent field-effect transistors have massive potential for future classical [1,2] and quantum computation [3] nanodevices. This is due to the recent experimental discovery that superconductivity in thin metallic films can be suppressed by externally applying a sufficiently strong external dc electric field, denoted $E_{\mathrm{cr,ext}}$ [4–27]. Experimental evidence has shown that external electric fields (EFs) on the order of $\sim 10^8$ V/m are required to suppress the supercurrent in metallic thin films with a thickness of around 20 nm [28]. Despite several recent theoretical approaches in the literature [29–36], the debate is still open, and a quantitative microscopic prediction of the measured EF values $E_{\mathrm{cr,ext}}$ needed to experimentally suppress the superconductivity in thin films is still lacking.

This paper presents an internally consistent mechanism for the supercurrent field effect in metallic thin films by quantitatively predicting the EF magnitude needed to suppress superconductivity in alignment with experimental values. It is grounded in Eliashberg's microscopic theory and considers the electrostatic aspects of EF penetration and its screening. For the first time, this theory can predict the critical field required to eliminate superconductivity in 10–30-nm thick thin films without requiring any adjustable parameters. This prediction matches quite closely with the values measured experimentally. This new insight may provide material design guidelines to optimize the supercurrent field effect. The impacts of structural disorder, sample geometry and thickness, and dielectric screening are quantitatively evaluated to fully predict the expected performance in gating of supercurrent-field-effect transistors.

II. MODEL ASSUMPTIONS

The model is entirely generic for metallic thin films and is based on the following physical assumptions:

(i) The metallic thin film is thin enough that its penetration depth is comparable to the thickness or at least an order of magnitude smaller. For example, with NbN thin films, one has a penetration depth of 4–5 nm [37], comparable to the film thickness of $\sim 10 - 30$ nm. This ensures that the exponentially decaying EF in the film is never identically zero inside the film (recall that an exponentially decaying function is identically zero only for $r \to \infty$).

(ii) Even a minimal local value of the EF can tilt the attractive potential, which keeps a Cooper pair together [38,39].

(iii) Following Cooper [39] and Weisskopf [40], we assume the attractive potential that keeps the two electrons bound in the Cooper pair to be a spherically symmetric well (*s*-wave bound state), cf. Fig. 1.

(iv) Then the Cooper pair, according to BCS theory [39,41], is governed by a Schrödinger equation for an *s*-wave bound state. In the presence of a small but finite electric field pointing along the (arbitrary) direction z, the stationary Schrödinger equation reads [38]

$$\left(\tfrac{1}{2}\nabla^2 + \mathcal{E} + u(r) - Ez\right)\psi = 0, \tag{1}$$

where $\mathcal{E}$ is the energy, E is the electric field magnitude, z is the spatial coordinate along which the EF points, and ψ is the wave function. In the above equation, atomic units are used. Furthermore, the attractive potential is schematically given by a spherical well: $u(r) = -\Delta$ for $0 \leqslant r \leqslant \xi$ and zero otherwise, where Δ is the BCS energy gap and ξ is the coherence length (cf. Fig. 1). The solutions to Eq. (1) are obtained by

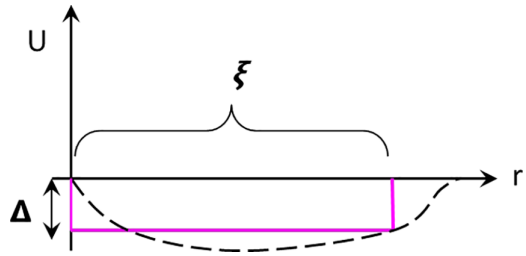

FIG. 1. Schematic of the potential energy profile experienced by an electron bound in a Cooper pair (in the absence of external fields), where r measures the radial distance from the other electron in the pair, following the original real-space description of Cooper pairs given by Weisskopf [40]. Therefore, the electron in a Cooper pair is effectively in a bound state of s-wave type. Applying a dc electric field to this s-wave bound state leads to field-induced electron tunneling, which escapes from the bound state with a probability w outlined in textbooks [38].

separating the variables in parabolic coordinates, and they can be found in textbooks [38]. From the solution to Eq. (1), one obtains the characteristic critical electric field magnitude $E_{\rm cr}$ to break the Cooper pair.

(v) We also assume that the coherence length ξ is less than the thickness of the film or, at most, comparable to the thickness of the film. This is because we treat the response of the superconducting phase as a whole; note that in experimentally realized thin films, the granularity and disorder could set the value of ξ much lower than in a bulk crystalline material. As we shall see, ξ is also essential to compute the critical field $E_{\rm cr}$.

The above assumptions can be applied to various materials and devices studied in the literature [28]. For all these materials, the measured values of the critical field $E_{\rm cr}$ always fall within the range $\sim 1 \times 10^8$ to $\sim 8 \times 10^8$ V/m.

III. STRUCTURE OF THE PAPER

In the following, we first summarize the microscopic Eliashberg theory framework used to quantitatively estimate the gap energy (Δ) for actual materials, which corresponds to the binding energy of Cooper pairs. Next, we mathematically describe the two electrons in the Cooper pair as being in an s-wave bound state subjected to an electric field. We then revisit the derivation of the field-assisted tunneling probability, which indicates how the s-wave bound state dissociates (depairing probability). From this solution, we derive an expression for the critical or characteristic value of the electric field (EF), $E_{\rm cr}$, necessary to dissociate the Cooper pair as a function of Δ and the coherence length ξ (which can be replaced by the mean free path ℓ in very disordered films). In the last part, we estimate the correction to the critical field due to the screening of the EF within the film thickness, examining the spatial decay of the EF from the surface into the film's interior. Consequently, we then calculate the actual value of the externally applied EF that should be applied to induce the suppression of superconductivity in the film, $E_{\rm cr,ext}$. The estimate is compared with the experimental data for the illustrative case of NbN thin films.

IV. QUANTITATIVE THEORY OF SUPERCONDUCTIVITY IN METALLIC THIN FILMS

A. Eliashberg equations

We resort to Eliashberg theory to compute the BCS energy gap of a given material and the coherence length. The standard (infinite) one-band s-wave Eliashberg equations, when the Migdal theorem holds [42], are given in terms of the renormalization function $Z(i\omega_n)$ and the gap function $\Delta(i\omega_n)$ as [43–49]

$$\Delta(i\omega_n)Z(i\omega_n) = \pi T \sum_{\omega_{n'}} \frac{\Delta(i\omega_{n'})}{\sqrt{\omega_{n'}^2 + \Delta^2(i\omega_{n'})}} \times [\lambda(i\omega_{n'} - i\omega_n) - \mu^*(\omega_c)\theta(\omega_c - |\omega_{n'}|)] \quad (2)$$

$$Z(i\omega_n) = 1 + \frac{\pi T}{\omega_n} \sum_{\omega_{n'}} \frac{\omega_{n'}}{\sqrt{\omega_{n'}^2 + \Delta^2(i\omega_{n'})}} \lambda(i\omega_{n'} - i\omega_n), \quad (3)$$

where $\theta(\omega_c - |\omega_{n'}|)$ is the Heaviside function, ω_c is a cutoff energy ($\omega_c > 3\Omega_{\rm max}$, where $\Omega_{\rm max}$ is the maximum phonon energy) [45], $\mu^*(\omega_c)$ is the Coulomb pseudopotential, and $\lambda(i\omega_{n'} - i\omega_n)$ is a function related to the electron-boson spectral density $\alpha^2F(\Omega)$ through the relation

$$\lambda(i\omega_n' - i\omega_n) = 2\int_0^\infty \frac{\Omega\,\alpha^2F(\Omega)}{\Omega^2 + (\omega_{n'} - \omega_n)^2} d\Omega. \quad (4)$$

The strength of the electron-phonon coupling intensity is given by the electron-phonon coupling parameter $\lambda = 2\int_0^\infty \frac{\alpha^2F(\Omega)\,d\Omega}{\Omega}$.

The Eliashberg equations are usually solved numerically using an iterative method until numerical convergence is achieved. The numerical procedure is simple when formulating it on the imaginary axis, but much less so for the real axis. The critical temperature T_c can be calculated by solving an equation of eigenvalues or, more efficiently, by assigning a minimal test value to the superconducting gap. For example, for Pb, it is $\Delta = 1.34$ meV at $T = 0$ K; then we fix $\Delta(T^*) = 10^{-10}$ meV and compute the temperature T^* at which the solution converges to find $T_c = T^*$. This method achieves a precision in the T_c value significantly higher than the experimental confidence interval.

Suppose that one removes the approximations of the infinite bandwidth and takes the density of states (DOS) equal to a constant (i.e., its value at the Fermi level). This situation arises when we consider the effect of thickness in a thin film [50] (see Appendix). In that case, we can still solve the problem considering the quantum confinement correction for thin films, but the Eliashberg equations are slightly more complex, becoming four equations [45]. However, assuming the DOS to be symmetrical with respect to the Fermi level, $N(\varepsilon) = N(-\varepsilon)$, the situation simplifies again because the nonzero self-energy terms remain only two, i.e., just a generalization of the equations discussed before for $Z(i\omega_n)$ and $\Delta(i\omega_n)Z(i\omega_n)$.

In such a case, they read [51,52]

$$\Delta(i\omega_n)Z(i\omega_n) = \pi T \sum_{\omega_{n'}} \frac{\Delta(i\omega_{n'})}{\sqrt{\omega_{n'}^2 + \Delta^2(i\omega_{n'})}} \left[\frac{N(i\omega_{n'}) + N(-i\omega_{n'})}{2}\right] \times [\lambda(i\omega_{n'} - i\omega_n) - \mu^*(\omega_c)\theta(\omega_c - |\omega_{n'}|)] \frac{2}{\pi} \arctan\left(\frac{W}{2Z(i\omega_{n'})\sqrt{\omega_{n'}^2 + \Delta^2(i\omega_{n'})}}\right), \tag{5}$$

$$Z(i\omega_n) = 1 + \frac{\pi T}{\omega_n} \sum_{\omega_{n'}} \frac{\omega_{n'}}{\sqrt{\omega_{n'}^2 + \Delta^2(i\omega_{n'})}} \left[\frac{N(i\omega_{n'}) + N(-i\omega_{n'})}{2}\right] \lambda(i\omega_{n'} - i\omega_n) \times \frac{2}{\pi} \arctan\left(\frac{W}{2Z(i\omega_{n'})\sqrt{\omega_{n'}^2 + \Delta^2(i\omega_{n'})}}\right), \tag{6}$$

where $N(\pm i\omega_{n'}) = N[\pm Z(i\omega_{n'})\sqrt{(\omega_{n'})^2 + \Delta^2(i\omega_{n'})}]$ and the bandwidth W is equal to half the Fermi energy, $E_F/2$. Furthermore, a symmetric DOS is also beneficial in obtaining faster and simpler numerical convergence.

B. Comparison with experimental data for the T_c

The theory above has recently been shown to provide a quantitative, parameter-free prediction of the superconducting critical temperature in actual thin-film materials, such as Pb and Al thin films [50]. We can now compare the predicted values of this theory of T_c with experimental data, particularly for NbN thin films. The Eliashberg equations mentioned above are solved using the experimentally determined Eliashberg spectrum $\alpha^2F(\Omega)$ found in Ref. [53], along with the concentration of free carriers as a function of film thickness, as reported in the literature [54]. This leaves no adjustable parameters for comparison. The theoretical predictions are compared with the experimental data from Ref. [54]. Without any adjustable parameters, the theory aligns excellently in quantitative terms with the experimental data for $L = 20$ nm, predicting a T_c value of 16.1 K. In what follows, we will concentrate our estimates on films of this thickness or similar. Regarding the possible effects of the electrostatic field on the Coulomb pseudopotential μ^*, this problem has been previously addressed in [55]. There, it was found that the effects of the electrostatic field on μ^* are very small and practically negligible, leading to a variation in the corresponding T_c of just 0.0027%.

V. ELECTRIC-FIELD-INDUCED COOPER PAIR SPLITTING

The issue of splitting a Cooper pair by an electric field is similar to the classic problem of electric-field-induced dissociation of an s-wave bound state. This similarity arises because, within BCS theory, a Cooper pair is represented as an s-wave bound state that satisfies the Schrödinger equation for two electrons interacting through an effective attractive force [39,41], with a real-space description initially proposed by Weisskopf and illustrated schematically in Fig. 1. The solution for bound-state dissociation in an electric field is well known [38] and has already been applied to the context of Cooper pair splitting by an external electric field in Refs. [56,57]. The formula for the critical electric field magnitude needed to split the Cooper pair is given by

$$E_{\rm cr} = \frac{2\Delta}{e\,\xi}, \tag{7}$$

where Δ is the energy gap obtained by the solution of Eliashberg equations, e is the electron charge, and ξ is the coherence length, which is self-consistently obtained by the solution of Eliashberg equations (Sec. IV and [58]):

$$\xi(T) = \frac{v_F}{2} \frac{\sum_n \frac{\Delta^2(i\omega_n)}{Z(i\omega_n)[\omega_n^2 + \Delta^2(i\omega_n)]^{1.5}}}{\sum_n \frac{\Delta^2(i\omega_n)}{\omega_n^2 + \Delta^2(i\omega_n)}}. \tag{8}$$

The above estimate for $E_{\rm cr}$ can be obtained by considering Eq. (1), i.e., the Schrödinger equation for an electron initially bound to a s-wave bound state (the Cooper pair) of energy depth Δ, and subjected to an external electric field of magnitude $E = |-\nabla V|$. While the s-wave bound state (the Cooper pair) is spherically symmetric, the electric field is directed along a specific spatial direction, which could be any direction in the solid angle. In analogy to what is shown in the textbooks (Ref. [38], pp. 296–297), one solves the Schrödinger equation (1) in parabolic coordinates and uses the solution to compute the probability current of the electron escaping away from the bound state in the direction of the EF [i.e., the coordinate z in Eq. (1)]. The result for the probability w of the electron tunneling away from a bound state is given in dimensionless form as [38]

$$w \sim \exp\left(-\frac{2}{3E}\right), \tag{9}$$

where E is the nondimensionalized electric field's magnitude (absolute value). For an s-wave bound state of unitary depth energy and unitary radius, converting to a dimensionful form, the above formula from [38] reads

$$w \sim \exp\left(-\frac{2}{3}\frac{E_a}{E}\right), \tag{10}$$

where $E_a = 2R_H/ea_0$, with R_H the Rydberg energy and a_0 the Bohr radius. In particular, one finds that the critical electric field scale to dissociate the bound state is given by

$$E_{\rm cr} = \frac{2R_H}{ea_0}. \tag{11}$$

The same result is valid for a generic bound state of depth energy Δ and range ξ, leading to [35]

$$E_{\rm cr} = \frac{2\Delta}{e\xi}. \tag{12}$$

It is important to note that the direction z of the electric field in Eq. (1), in principle, does not affect the critical value $E_{\rm cr}$, because only the absolute value of the electric field, $E = |-\nabla V|$, appears in the solution for the escape probability [38]. However, the anisotropic lattice structure may still be important and could affect the effective value of the electric field in the sample. For example, if one takes our Eq. (1) as the starting point, and assuming that the bound state remains an s-wave, the structural anisotropy of the lattice can affect the final result for $E_{\rm cr}$ through the effective value of E. In turn, this will depend on the crystallographic orientation of the sample with respect to the direction, z, of the incident electric field. Indeed, this may lead to a different penetration of the electric field, hence to a different average value of E in the sample, depending on whether the field direction z is aligned with the c crystallographic axis (hence orthogonal to the crystallographic layered plane ab) or if it lies in the ab layered plane. This is an important aspect that should be considered for experimental design.

In the above equation, the spatial extent or range of the bound state is denoted with ξ. For the case of a Cooper pair, this is equal to the coherence length [40]; cf. Fig. 1. The coherence length (ξ) may depend on the material and is given by [59]

$$\frac{1}{\xi} = \frac{1}{\xi_0} + \frac{1}{\ell}, \tag{13}$$

where ξ_0 is the intrinsic (Pippard) coherence length, and ℓ is the mean free path. Thin films, such as those used in the supercurrent field-effect devices, have a microstructure characterized by microcrystallites that limit the values of ℓ. Since, typically, $\ell \ll \xi_0$ (because ξ_0 can be tens or hundreds of nanometers), the coherence length ξ is controlled by ℓ, and hence by the disorder, and $\xi \approx \ell$. For experimental metallic thin-film systems, the disorder is indeed always present [60], and we can safely assume $\xi \approx \ell$. Therefore,

$$E_{\rm cr} = \frac{2\Delta}{e\,\ell}. \tag{14}$$

Being in the diffusive regime, the coherence length ℓ has a small value, not that of a bulk superconductor but that of a thin film. From our theory presented in Secs. IV A and IV B, we know the gap energy Δ for a given material, and we can estimate the critical electric field $E_{\rm cr}$ for the suppression of superconductivity inside the film under the assumptions stated in Sec. II.

For the example of NbN, the critical electric field values needed to suppress the superconductivity in 10–30-nm thick thin films are on the order of 10^7 V/m, under the assumption of no screening. More precisely, at $0 < T < 8$ K, the value is calculated on the basis of Eq. (14) with $\ell = 3.96$ Å, and Δ, evaluated from the Eliashberg theory, is practically constant with temperature and produces a value of critical field $E_{\rm cr} = 1.4 \times 10^7$ V/m. This estimate is one order of magnitude lower than the experimental values of $\sim 10^8$ V/m reported in the literature for films of comparable thickness [28].

As mentioned, this estimate still assumes a perfect external electric field penetration to the sample. In other words, it does not consider the screening of the EF within the sample. The screening effects must be taken into account in order to determine the magnitude of the external EF required to suppress superconductivity, a process detailed in the next section.

VI. CRITICAL ASSESSMENT OF THE ELECTRIC FIELD REQUIRED TO INHIBIT SUPERCONDUCTIVITY IN THIN FILMS

A. Average field within the sample

In our theoretical estimate of the critical electric field $E_{\rm cr}$ required to suppress superconductivity, as presented in the previous section, we implicitly assumed that the strength of the EF that acts to separate Cooper pairs inside the film is identical to that of the externally applied electric field. However, it is clear that the magnitude of the EF within the thin film is significantly lower than that of the external EF and exhibits spatial heterogeneity because of the penetration profile. We will address these issues to develop a comprehensive quantitative prediction for superconductivity suppression throughout the thin film.

The magnitude of the EF in the thin film is significantly lower than the external EF due to screening. Here, we evaluate this reduction, which allows us to estimate $E_{\rm cr,ext}$, the externally applied EF magnitude necessary to suppress superconductivity.

Regarding the penetration of static and quasistatic electric fields into the superconducting phase of the material—and especially the temperature dependence thereof—this remains an open issue in our understanding of superconductivity [61–70], which we cannot address here.

In place of a conclusive theory, which would typically require, at least, the simultaneous numerical solution of several coupled differential equations—the Schrödinger equation, the Ginzburg-Landau equation, the Maxwell equations, and the Poisson equation [31,32,71,72]—here we use empirical input from *ab initio* simulations and experiments of Piatti *et al.* [37] for the same example of NbN thin films discussed above. According to that reference, the penetration depth of the electric field into NbN superconducting thin films is significantly greater than what is predicted by Thomas-Fermi estimates and other standard screening theories of (normal) metals, which typically measure just a few angstroms in the range from 0.5 to 3 nm.

According to the screening theory of normal metals [73], see also [74–76], the electric field incident onto the surface of a metal decays exponentially from the value it has at the interface. Denote by E_0 the value of the EF at the interface between the metal and the surrounding environment, and by $x = 0$ the coordinate of the interface. Hence, $E_0 \equiv E\ (x = 0)$.

We assume, for simplicity, that E_0 coincides with the magnitude of the external EF as determined in the experiment. We used a common semiempirical form for the profile of the EF inside the sample from Ref. [74], which finds its justification from electrodynamics [66,73]:

$$E(x) = E_0 \exp(-x/l), \tag{15}$$

where l is a characteristic penetration lengthscale. For NbN in the superconducting state, this length is large (compared to normal metals), that is, $l \approx 0.5$–3 nm, as shown in [37]. In agreement with the experimental protocol [4,5], we assume a bipolar setup in which the EF is incident on both sides (surfaces) of the film. This implies that the EF is exponentially decaying within the film from its external value E_0, on both sides at $z = 0$ and $z = L$ [77]. Hence, we have complete symmetry across the midline $z = L/2$ plane of bilateral symmetry. This simplifies our problem, as we only need to consider the exponential decay on one side of the film. We can safely assume that the superconductor "sees" the inhomogeneous electric field mediated on the scale of at least ξ. However, it is assumed that the thickness of the film is not larger than the coherence length. We can thus estimate the "effective" electric field as the average magnitude of the EF inside the whole sample as

$$\bar{E} = \frac{1}{L/2}\int_0^{L/2} E_0\, e^{-x/l} dx = E_0 \frac{2l}{L}(1 - e^{-L/(2l)}). \tag{16}$$

In this formula, E_0 represents the external EF incident on the surface of the film, while $\bar{E}$ represents the average value of the EF seen by the superconductor inside the film.

We should also briefly remark on the fact that the material, in its normal state, behaves like a metal under a dc electric field. Static electric fields of magnitude 10^8 V/m, such as those considered in our work, are below the typical values ($\sim 10^9$ V/m) which induce field-emission, or other nonlinear and quantum effects (arcing, surface plasmon, and charge instabilities). Thus, all these situations can be safely ruled out. The penetration length in the normal state does not change significantly under the applied EF, at least according to the available evidence [37,78], and in general this is expected to be determined by the equilibrium electron properties (DOS, etc.), which are not strongly modified by the static EF, again unless the EF is so extreme as to cause significant nonlinear or quantum effects (e.g., field emission, tunneling), which is not the case for our systems. For an estimate of the polarization induced by the electric field in the normal state, we consider the induced surface charge density: $\sigma = \epsilon_0 E = (8.85 \times 10^{-12}) \times (10^8) = 8.85 \times 10^{-4}$ C/m^2. In our model, the electric field is sufficiently strong to induce a small correction of the electrical field penetration depth as confirmed by DFT computations [37]. However the penetration depth still involves just only a few atomic layers at the surface, so it does not significantly affect the screening mechanism at the macroscopic level.

B. Magnitude of the external electric field required to suppress superconductivity

Using the empirical data from [37] for the example of NbN, we select a screening length of $\ell = 1$ nm. With this choice, we can estimate the magnitude of the electric field EF that must be applied externally to break Cooper pairs in the presence of dielectric screening within the film. The magnitude of the EF must be sufficient to ensure that the average electric field $\bar{E}$ inside the sample is equal to the critical value $E_{\rm cr}$, which is necessary to break Cooper pairs. This critical value is calculated using Eq. (14) and Eliashberg's theory discussed in Sec. V. Hence, we must set $\bar{E}$ in Eq. (16) equal to $E_{\rm cr}$ evaluated in Sec. V, and solve for E_0, the value we supply externally to suppress the superconductivity. Let us call this value $E_0 \equiv E_{\rm cr,ext}$ to distinguish it from $E_{\rm cr}$ used before. The magnitude of EF that has to be supplied externally is thus given by

$$E_{\rm cr,ext} = \frac{E_{\rm cr}}{\frac{2l}{L}(1 - e^{-L/(2l)})} = \frac{2\Delta/e\,\ell}{\frac{2l}{L}(1 - e^{-L/(2l)})}. \tag{17}$$

This equation represents one of the most important results in this paper. It establishes a direct quantitative relationship between the magnitude of the externally applied electric field, $E_{\rm cr,ext}$, and several physical parameters that are specific to the material and the sample: Δ (material-dependent), ℓ (material-dependent), l (material-dependent), and L (sample geometry).

The final result for the EF magnitude, $E_{\rm cr}$, that has to be supplied externally to cause the suppression of superconductivity in a thin film NbN of $L = 20$ nm thick, calculated according to Eq. (17) with $l = 1$ nm [37,78], is

$$E_{\rm cr,ext} = 1.45 \times 10^8 \text{ V/m}. \tag{18}$$

We recall that to obtain this value, the energy gap Δ in Eq. (17) was computed in Sec. IV through Eliashberg's theory for NbN using an Eliashberg spectral function $\alpha^2 F(\Omega)$ obtained experimentally. The latter includes structural disorder effects, which are ubiquitous in experimental thin films.

It turns out that the value of the EF to be supplied is about $\sim 10^8$ V/m, which is in excellent agreement with the values measured experimentally [28]. Choosing a lower value of the screening length l such as $l < 1$ nm within the range reported in [37,78] would lead to values of the critical electric field somewhat more significant than 1×10^8 V/m but still of the same order of magnitude and ideally in line with the experimental data in the literature [28]. In the above estimate, we have used a screening length value, l, which is temperature-independent. We will postpone discussing the trend of $E_{\rm cr}$ versus T until future studies when a comprehensive theory of the temperature dependence of l in the superconducting phase will be available.

In the above model, the choice of the screening length, l, plays an important role. In addition to direct experimental measurements, the screening length l can also be estimated by standard DFT calculations, as done in [78]. In practice, one can use the QUANTUM ESPRESSO package and then solve the Kohn-Sham equations for the charge density. In the case of NbN, this approach yielded penetration depths in good agreement with the experimental values. In addition to the *ab initio* approach, a different pathway could be based on estimating the density of free electrons and then using this as input in a de Gennes jellium-type framework for the dielectric response such as the one described recently in [79].

VII. GENERAL MECHANISM OF SUPERCURRENT SUPPRESSION OVER THE WHOLE SAMPLE

A. Bipolarity

The mechanism and calculations described above are "bipolar" in that they do not depend on the polarity of the applied electric field as long as a nonzero local EF is acting on the Cooper pair. According to Eq. (1), the EF's local direction (z) is irrelevant since the s-wave bound state is spherically symmetric. In our mathematical model, we assumed that the density of states is symmetric concerning the Fermi level, which makes the calculations perfectly bipolar. This assumption approximates good metals where the Fermi level is relatively high because of the flattening of the Fermi square-root DOS at higher energies. Additionally, this approximation simplifies the numerical solutions to the Eliashberg equations, significantly reducing computational time. If we had not made this assumption, a slightly asymmetric DOS would have resulted in a minor deviation from bipolarity in the mechanism. However, this effect would be negligible for metals, especially in comparison to the experimental data. However, this is an interesting point that we plan to revisit in future studies.

B. Effects on the resistivity

The investigation of the effects of an electrostatic field on superconductors is a long-standing issue [80]. In the normal state, conductivity can be weakly modified, and with respect to the superconducting phase, the transition temperature can be either (weakly) positively or negatively shifted. Highly accurate measurements taken in the superconducting transition region for indium films [80] consistently showed that negative charging (that is, adding electrons) leads to an increase in resistance, while positive charging (i.e., removing electrons) results in a corresponding decrease in resistance. When subjected to an electrostatic field of approximately 10^7 V/m, the effects are minimal, producing a transition temperature shift of the order of 10^{-4} K.

This effect can be explained using a generalization of the proximity effect in Eliashberg's theory [81,82], employing a model with no free parameters [83]. In all the cases examined (i.e., lead [55], indium [83], and magnesium diboride [84]), the effect is minimal. In Eliashberg's theory, the relevant parameter is the electron-phonon spectral function $\alpha^2F(\Omega)$, which displays a very weak dependence on the presence of electrostatic fields at this intensity. The same holds in Allen's theory [85], which is used to calculate the resistivity as a function of temperature and is connected to Eliashberg's theory. In this context, the electron-phonon transport spectral function $\alpha^2F_{\rm tr}(\Omega)$ emerges, which is closely related to the Eliashberg spectral function $\alpha^2F(\Omega)$ in the superconducting state [85]. Likewise, in this scenario, electrostatic fields of this intensity alter the electron-phonon transport spectral function almost imperceptibly; thus, the effects are also minimal. Because these two functions are also linked to the value of the DOS at the Fermi level, the minor variations in the critical temperature and resistivity depend on the direction of the applied electrostatic field because the normal DOS may be asymmetric relative to the Fermi level.

VIII. "MATERIALS BY DESIGN" GUIDELINES

A. Standard thin films with $L > 10$ nm

A fundamental result of this paper is Eq. (17), which provides a possible microscopic estimate of the externally applied electric field needed to suppress superconductivity in thin films as a function of key physical parameters that depend on the material and/or the sample preparation. In addition to offering a quantitative prediction of the critical field $E_{\rm cr,ext}$ in agreement with experimental data, this formula presents new guidelines for materials design. For example, the impact of structural disorder will influence both Δ and ℓ. The influence of disorder on Δ parallels its effect on T_c, and is notably complex and dependent on the material and sample [86,87]. In the standard s-wave Eliashberg theory, of course, the disorder does not affect T_c and Δ, but this is no longer true in the generalized Eliashberg theory. Furthermore, in the case of an intense disorder, the spectral function and the Coulomb pseudopotential can change. In some materials, the disorder will increase T_c and, consequently, Δ; in others, it will cause a decrease. In other materials, the effect can be nonmonotonic, exhibiting either a dome or a minimum (for example, for Pb-based alloys, T_c exhibits a minimum as a function of disorder [87]). In contrast, we anticipate that the mean free path ℓ will decrease consistently as the disorder increases [59]. Thus, Eq. (17) predicts various scenarios in which one should optimize the disorder dependence of the ratio Δ/ℓ. For example, to reduce the critical field $E_{\rm cr,ext}$, it is advisable to adjust the structural disorder to minimize the ratio Δ/ℓ.

We note that the value of $E_{\rm cr,ext}$ also depends on the thickness of the film. Specifically, since $L \gg l$, the exponential in the formula becomes a small number compared to 1; therefore, the primary effect of decreasing L is to decrease the critical field $E_{\rm cr,ext}$.

Finally, the effect of the penetration depth of the EF l on the critical field is quite clear: once again, because $L \gg l$, the primary consequence of increasing l will be a reduction in the critical field $E_{\rm cr,ext}$. Generally, the screening penetration depth would be more significant for low-density superconductors. However, while this is evident from Eq. (17), it is certainly not straightforward to determine how to achieve this kind of fine-tuning in materials engineering, given the current lack of microscopic insight into the dielectric screening in the superconducting phase of metals.

B. Ultrathin films with $L < 10$ nm

The above illustrative calculation for NbN thin films was done in a regime where the energy gap Δ is independent of the film thickness. However, several common-use materials, including Al and Pb, exhibit a strong dependence of their T_c and Δ on the thickness L when L approaches the 2D limit [50,88,89]. These effects may already become important at $L < 10$ nm, and the film thickness, which marks the onset of these effects, varies (increases) with the concentration of free carriers in the material. In most cases, T_c and therefore Δ increase markedly as the film thickness L decreases, as observed experimentally [90–92], although sometimes a maximum is also observed in T_c versus L [93,94] with a regime where

T_c grows with L. The recently developed Eliashberg theory corrected for quantum confinement [50] can quantitatively describe these effects without free parameters [50].

The quantum confinement corrections to the Eliashberg theory amount to having a thickness-dependent Fermi energy, $E_F(L)$, and an electron DOS which is also thickness-dependent, $N(\epsilon;L)$. The specific functional forms of these dependencies can be found in Refs. [50,88] and are summarized in Appendix. All this implies that the energy gap $\Delta(L)$ entering Eq. (17) for the critical magnitude of the EF will also become a function of the thickness of the film L. Therefore, for ultrathin films, Eq. (14) should be replaced by

$$E_{\mathrm{cr,ext}} = \frac{2\Delta(L)/e\,\ell}{\frac{2l}{L}(1-e^{-L/(2l)})}, \tag{19}$$

with an explicit dependence of Δ on L due to quantum confinement effects. Generally, knowing $\Delta(L)$ from the theory [50], one can minimize the function $E_{\mathrm{cr,ext}}(L)$ defined by the above Eq. (19) to identify the thickness value corresponding to the lowest critical EF required to suppress superconductivity in this regime.

IX. CONCLUSIONS

In conclusion, we have presented a possible route to a microscopic quantitative theory of electrostatic field-driven superconductivity suppression in thin films. The theoretical model treats the Cooper pair as an s-wave bound state (following the original description by Cooper [39]), which is subjected to a small but nonvanishing electric field within the film. Using the Schrödinger equation solution for s-wave bound state dissociation through electric-field-assisted tunneling, we derive an expression for the critical or characteristic electric field magnitude inside the film to break the Cooper pairs, thus suppressing superconductivity. This critical electric field is proportional to the ratio between the superconducting energy gap value Δ and the coherence length ξ, as shown in Eq. (7). The gap value is related to the T_c value through the BCS relation $2\Delta/k_BT_c \approx 3.53$. However, in our framework, we computed it via the most accurate Eliashberg theory, which considers structural and disorder effects on the phonon spectral function for a specific material, achieving quantitative agreement with experimental data for the behavior of T_c without any adjustable parameters.

Because the T_c values of the materials used in the experiments [28] are comparable, so are the energy gaps Δ. Regarding the coherence length ξ, it should be noted that the experiments are typically in the diffusive limit for many materials. Therefore, we need to consider the coherence length value obtained from Eq. (13), as the mean free path ℓ is always relatively small in real materials and of the same order of magnitude in all experimental cases studied in the literature [28]. Generally speaking, ξ is typically the same for most materials investigated experimentally to date [28]; therefore, the critical field value primarily depends on the energy gap value Δ.

The outcome of the theory is given by Eq. (17), which provides a quantitative estimate of the critical field required to suppress superconductivity, as it relates to all key microscopic parameters dependent on material and sample: energy gap Δ, mean free path ℓ, film thickness L, and EF screening length in the superconducting phase l.

Focusing on the 20-nm-thick NbN films, for which the theory provides a perfect quantitative prediction of Δ, we used Eq. (17) to compute the critical electric field required to break up Cooper pairs and suppress superconductivity. Based on our calculation of Eliashberg's theory for realistic NbN films, and considering the spatially decaying profile of the electric field within the sample, our theory predicts a critical field $E_{\mathrm{cr}} \approx 1.45 \times 10^8$ V/m, which aligns well with the experimentally measured values of $\sim 10^8$ V/m [28]. Combined with the underlying electrostatic model, these calculations provide a comprehensive understanding of the electric-field-driven suppression of superconductivity in metallic thin films. This understanding accounts for the inhomogeneous distribution of the electric field within the sample as a result of dielectric screening in the superconducting phase.

The theory is very general and extends beyond this specific calculation as it applies to all thin films made of conventional materials. It also accounts for the dependence on film thickness due to quantum confinement in the ultrathin film regime ($L < 10$ nm), where the energy gap varies significantly with thickness [50,88,89]. This could explain the experimental data related to measurements of films with varying thicknesses up to the quasi-2D limit. These new insights and understandings may enable us to deliberately adjust the supercurrent field effect in gating and nanoelectronic devices based on superconductors.

ACKNOWLEDGMENTS

A.Z. gratefully acknowledges funding from the European Union through Horizon Europe ERC Grant No. 101043968 "Multimech," from the U.S. Army Research Office through Contract No. W911NF-22-2-0256, and from the Niedersächsische Akademie der Wissenschaften zu Göttingen in the frame of the Gauss Professorship program. F.G. acknowledges the EU's Horizon 2020 Research and Innovation Framework Programme under Grants No. 964398 (SUPERGATE), No. 101057977 (SPECTRUM), and the PNRR MUR project PE0000023-NQSTI for partial financial support. A.B acknowledges MUR-PRIN 2022–Grant No. 2022B9P8LN-(PE3)-Project NEThEQS "Non-equilibrium coherent thermal effects in quantum systems" in PNRR Mission 4 - Component 2 - Investment 1.1 "Fondo per il Programma Nazionale di Ricerca e Progetti di Rilevante Interesse Nazionale (PRIN)" funded by the European Union - Next Generation EU and the PNRR MUR project PE0000023-NQSTI and CNR project QTHERMONANO.

DATA AVAILABILITY

No data were created or analyzed in this study.

APPENDIX: ELECTRON CONFINEMENT MODEL AND CALCULATION DETAILS

This Appendix summarizes how the electronic DOS and Fermi energy depend on the film thickness L via the relations derived from the free-electron confinement model for thin

films of Ref. [88] and quantitatively verified compared with the experimental data in Ref. [50]. In the calculations presented in the main article, the effect of film thickness on DOS is practically negligible since they are only set for ultrathin films with thickness $L < 10$ nm. However, for completeness, the dependencies on L are made explicit.

When the system is confined along one of the three spatial directions, such as in thin films, the DOS cannot be approximated by a constant but takes a different form [50,88]. In this case, we have two different regimes depending on the thickness of the film L: In the first confinement regime, when $L > L_c$ and $E_F > \varepsilon^*$, the DOS has the following form: $N(\varepsilon) = N(0)C[\vartheta(\varepsilon^* - \varepsilon)\sqrt{\frac{E_F}{\varepsilon^*}}\frac{|\varepsilon|}{E_F} + \vartheta(\varepsilon - \varepsilon^*)\sqrt{\frac{|\varepsilon|}{E_F}}]$, where $C = (1 + \frac{1}{3}\frac{L_c^3}{L^3})^{1/3}$, $\varepsilon^* = \frac{2\pi^2\hbar^2}{mL^2}$, $L_c = (\frac{2\pi}{n_0})^{1/3}$, m is the electron mass, L is the thickness of the film, n_0 is the carrier density, and $E_{F,\mathrm{bulk}}$ is the Fermi energy of the bulk material. In this case, it is possible to demonstrate [88] the following relations:

$$E_F = C^2 E_{F,\mathrm{bulk}}, \tag{A1}$$

$$N(E_F) = CN(E_{F,\mathrm{bulk}}) = CN(0), \tag{A2}$$

$$N(E_{F,\mathrm{bulk}}) = \frac{V(2m)^{3/2}}{2\pi^2\hbar^3}\sqrt{E_{F,\mathrm{bulk}}}. \tag{A3}$$

In the second confinement regime, $L < L_c$, the DOS has a new linear dependence on the energy, in contrast to the standard square-root dependence [88].

In summary, in this version of the Eliashberg theory, four things have been modified to account for the effect of free-electron confinement in thin films:

(a) The DOS will no longer be a constant but a function of energy. We removed the factors C because we put this factor in the renormalization of the electron-phonon interaction, so the density of states that we put in the Eliashberg equations in the first confinement regime $L > L_c$ is

$$N(\varepsilon) = \left[\vartheta(\varepsilon^* - \varepsilon)\sqrt{\frac{E_F}{\varepsilon^*}}\frac{|\varepsilon|}{E_F} + \vartheta(\varepsilon - \varepsilon^*)\sqrt{\frac{|\varepsilon|}{E_F}}\right]. \tag{A4}$$

(b) The electron-phonon interaction will be renormalized to have a new $\lambda(L) = C\lambda^{\mathrm{bulk}}$ to scale the electron-phonon spectral function without changing its shape. We moved the factor of normal DOS C within the definition of electron-phonon coupling as in the Coulomb pseudopotential. Of course, the reason for this choice is only pedagogical because, in this way, we can justify the use of the Allen-Dynes equation [95] for T_c, which is a crude but effective approximation of the numerical solution of the Eliashberg equations.

(c) The value of the Fermi energy will be renormalized in the following way: $E_F(L) = C^2 E_{F,\mathrm{bulk}}$. Furthermore, in the Eliashberg equations, it is $W = E_F/2$ in the symmetric case discussed above.

(d) The Coulomb pseudopotential changes (also the Fermi energy in the definition changes):

$$\mu^*(\omega_c, L) = \frac{C\mu_{\mathrm{bulk}}}{1 + \mu_{\mathrm{bulk}}\ln(E_F/\omega_c)},$$

$$\text{where} \quad \mu_{\mathrm{bulk}} = \frac{\mu^*_{\mathrm{bulk}}(\omega_c)}{1 - \mu^*_{\mathrm{bulk}}(\omega_c)\ln(E_{F,\mathrm{bulk}}/\omega_c)}.$$

In the second confinement regime, when $L < L_c$ and $E_F < \varepsilon^*$ [88],

$$N(\varepsilon) = C'N(0)\sqrt{\frac{E_F}{\varepsilon^*}}\frac{\varepsilon}{E_F}, \tag{A5}$$

where

$$N(\varepsilon = E_F) = C'N(0),$$

$$E_F(L) = \frac{\hbar^2}{m}\sqrt{\frac{(2\pi)^3 n_0}{L}} = C'^2 E_{F,\mathrm{bulk}},$$

$$C' = \frac{2}{6^{1/3}}\sqrt{\frac{L}{L_c}}.$$

In this confinement regime ($L < L_c$), the DOS is given by [88] $N(\varepsilon) = \sqrt{\frac{E_F}{\varepsilon^*}}\frac{|\varepsilon|}{E_F}$, and the factor C' goes to renormalize the electron-phonon coupling and the Coulomb pseudopotential as follows:

$$\lambda(L) = C'\lambda^{\mathrm{bulk}}, \quad \mu^*(\omega_c, L) = \frac{C'\mu_{\mathrm{bulk}}}{1 + \mu_{\mathrm{bulk}}\ln(E_F/\omega_c)}. \tag{A6}$$

Recalling that in the Eliashberg equations the reference energy is the Fermi energy taken as the zero of the energy, in the program that numerically solves the Eliashberg equations, the DOS has been rescaled in the following way (by also taking care that the DOS is continuous for $\varepsilon = \varepsilon^*$). When $L > L_c$ and $\varepsilon^* < E_F$,

$$N(\varepsilon) = \left[\vartheta(\varepsilon^* - \varepsilon)\sqrt{\frac{E_F}{E_F - \varepsilon^*}}\left(1 - \frac{|\varepsilon|}{E_F}\right) + \vartheta(\varepsilon - \varepsilon^*)\left(1 - \sqrt{\frac{|\varepsilon|}{E_F}}\right)\right]. \tag{A7}$$

Instead, when $L < L_c$ and $\varepsilon^* > E_F$,

$$N(\varepsilon) = \sqrt{\frac{E_F}{\varepsilon^*}}(1 - \frac{|\varepsilon|}{E_F}). \tag{A8}$$

Finally in our case for the illustrative calculation on the example of NbN, we have used $\lambda_{\mathrm{bulk}} = 1.46$, $\mu^*_{\mathrm{bulk}}(\omega_c) = 0.2522$ for $\omega_c = 180$ meV, $E_{F\mathrm{bulk}} = 12.418$ eV, $n_0 = 0.197 \times 10^{30}$ m^{-3}, $l = 0.4$ nm, and $v_F = 2.1 \times 10^6$ m/s.

[1] O. Mukhanov, D. Gupta, A. Kadin, and V. Semenov, Superconductor analog-to-digital converters, Proc. IEEE **92**, 1564 (2004).

[2] S. K. Tolpygo, Superconductor digital electronics: Scalability and energy efficiency issues (Review Article), Low Temp. Phys. **42**, 361 (2016).

[3] J. M. Gambetta, J. M. Chow, and M. Steffen, Building logical qubits in a superconducting quantum computing system, npj Quantum Inf. **3**, 2 (2017).

[4] G. De Simoni, F. Paolucci, P. Solinas, E. Strambini, and F. Giazotto, Metallic supercurrent in field-effect transistor, Nat. Nanotechnol. **13**, 802 (2018).

[5] G. De Simoni, F. Paolucci, C. Puglia, and F. Giazotto, Josephson field-effect transistors based on all-metallic Al/Cu/Al proximity nanojunctions, ACS Nano. **13**, 7871 (2019).

[6] F. Paolucci, G. De Simoni, P. Solinas, E. Strambini, N. Ligato, P. Virtanen, A. Braggio, and F. Giazotto, Magnetotransport experiments on fully metallic superconducting Dayem-bridge field-effect transistors, Phys. Rev. Appl. **11**, 024061 (2019).

[7] I. Golokolenov, A. Guthrie, S. Kafanov, Y. A. Pashkin, and V. Tsepelin, On the origin of the controversial electrostatic field effect in superconductors, Nat. Commun. **12**, 2747 (2021).

[8] F. Paolucci, F. Vischi, G. De Simoni, C. Guarcello, P. Solinas, and F. Giazotto, Field-effect controllable metallic Josephson interferometer, Nano Lett. **19**, 6263 (2019).

[9] T. Elalaily, O. Kürtössy, Z. Scherübl, M. Berke, G. Fülöp, I. E. Lukács, T. Kanne, J. Nygård, K. Watanabe, T. Taniguchi, P. Makk, and S. Csonka, Gate-controlled supercurrent in epitaxial Al/InAs nanowires, Nano Lett. **21**, 9684 (2021).

[10] M. Rocci, G. De Simoni, C. Puglia, D. D. Esposti, E. Strambini, V. Zannier, L. Sorba, and F. Giazotto, Gate-controlled suspended titanium nanobridge supercurrent transistor, ACS Nano **14**, 12621 (2020).

[11] J. Basset, O. Stanisavljević, M. Kuzmanović, J. Gabelli, C. H. L. Quay, J. Estève, and M. Aprili, Gate-assisted phase fluctuations in all-metallic Josephson junctions, Phys. Rev. Res. **3**, 043169 (2021).

[12] L. D. Alegria, C. G. Bøttcher, A. K. Saydjari, A. T. Pierce, S. H. Lee, S. P. Harvey, U. Vool, and A. Yacoby, High-energy quasiparticle injection into mesoscopic superconductors, Nat. Nanotechnol. **16**, 404 (2021).

[13] L. Bours, M. T. Mercaldo, M. Cuoco, E. Strambini, and F. Giazotto, Unveiling mechanisms of electric field effects on superconductors by a magnetic field response, Phys. Rev. Res. **2**, 033353 (2020).

[14] M. Rocci, D. Suri, A. Kamra, G. Vilela, Y. Takamura, N. M. Nemes, J. L. Martinez, M. G. Hernandez, and J. S. Moodera, Large enhancement of critical current in superconducting devices by gate voltage, Nano Lett. **21**, 216 (2021).

[15] M. F. Ritter, A. Fuhrer, D. Z. Haxell, S. Hart, P. Gumann, H. Riel, and F. Nichele, A superconducting switch actuated by injection of high-energy electrons, Nat. Commun. **12**, 1266 (2021).

[16] F. Paolucci, G. De Simoni, P. Solinas, E. Strambini, C. Puglia, N. Ligato, and F. Giazotto, Field-effect control of metallic superconducting systems, AVS Quantum Sci. **1**, 016501 (2019).

[17] G. Catto, W. Liu, S. Kundu, V. Lahtinen, V. Vesterinen, and M. Möttönen, Microwave response of a metallic superconductor subject to a high-voltage gate electrode, Sci. Rep. **12**, 6822 (2022).

[18] S. Yu, L. Chen, Y. Pan, Y. Wang, D. Zhang, G. Wu, X. Fan, X. Liu, L. Wu, L. Zhang *et al.*, Gate-tunable critical current of the three-dimensional niobium nanobridge Josephson junction, Nano Lett. **23**, 8043 (2023).

[19] G. De Simoni, C. Puglia, and F. Giazotto, Niobium dayem nanobridge Josephson gate-controlled transistors, Appl. Phys. Lett. **116**, 242601 (2020).

[20] H. Du, Z. Xu, Z. Wei, D. Li, S. Chen, W. Tian, P. Zhang, Y.-Y. Lyu, H. Sun, Y.-L. Wang *et al.*, High-energy electron local injection in top-gated metallic superconductor switch, Supercond. Sci. Technol. **36**, 095005 (2023).

[21] C. Puglia, G. De Simoni, and F. Giazotto, Electrostatic control of phase slips in Ti Josephson nanotransistors, Phys. Rev. Appl. **13**, 054026 (2020).

[22] T. Elalaily, M. Berke, M. Kedves, G. Fülöp, Z. Scherübl, T. Kanne, J. Nygård, P. Makk, and S. Csonka, Signatures of gate-driven out-of-equilibrium superconductivity in Ta/InAs nanowires, ACS Nano **17**, 5528 (2023).

[23] F. Paolucci, G. De Simoni, and F. Giazotto, A gate-and flux-controlled supercurrent diode effect, Appl. Phys. Lett. **122**, 042601 (2023).

[24] L. Ruf, T. Elalaily, C. Puglia, Y. P. Ivanov, F. Joint, M. Berke, A. Iorio, P. Makk, G. De Simoni, S. Gasparinetti *et al.*, Effects of fabrication routes and material parameters on the control of superconducting currents by gate voltage, APL Mater. **11**, 091113 (2023).

[25] L. Ruf, E. Scheer, and A. Di Bernardo, High-performance gate-controlled superconducting switches: large output voltage and reproducibility, ACS Nano **18**, 20600 (2024).

[26] P. Orús, V. M. Fomin, J. M. De Teresa, and R. Córdoba, Critical current modulation induced by an electric field in superconducting tungsten-carbon nanowires, Sci. Rep. **11**, 17698 (2021).

[27] J. Koch, C. Cirillo, S. Battisti, L. Ruf, Z. M. Kakhaki, A. Paghi, A. Gulian, S. Teknowijoyo, G. De Simoni, F. Giazotto *et al.*, Gate-controlled supercurrent effect in dry-etched Dayem bridges of non-centrosymmetric niobium rhenium, Nano Res. **17**, 6575 (2024).

[28] L. Ruf, C. Puglia, T. Elalaily, G. De Simoni, F. Joint, M. Berke, J. Koch, A. Iorio, S. Khorshidian, P. Makk, S. Gasparinetti, S. Csonka, W. Belzig, M. Cuoco, F. Giazotto, E. Scheer, and A. Di Bernardo, Gate control of superconducting current: Mechanisms, parameters, and technological potential, Appl. Phys. Rev. **11**, 041314 (2024).

[29] P. Solinas, A. Amoretti, and F. Giazotto, Sauter-Schwinger effect in a Bardeen-Cooper-Schrieffer superconductor, Phys. Rev. Lett. **126**, 117001 (2021).

[30] M. T. Mercaldo, P. Solinas, F. Giazotto, and M. Cuoco, Electrically tunable superconductivity through surface orbital polarization, Phys. Rev. Appl. **14**, 034041 (2020).

[31] P. Virtanen, A. Braggio, and F. Giazotto, Superconducting size effect in thin films under electric field: Mean-field self-consistent model, Phys. Rev. B **100**, 224506 (2019).

[32] L. Chirolli, T. Cea, and F. Giazotto, Impact of electrostatic fields in layered crystalline BCS superconductors, Phys. Rev. Res. **3**, 023135 (2021).

[33] M. T. Mercaldo, F. Giazotto, and M. Cuoco, Spectroscopic signatures of gate-controlled superconducting phases, Phys. Rev. Res. **3**, 043042 (2021).

[34] A. Amoretti, D. K. Brattan, N. Magnoli, L. Martinoia, I. Matthaiakakis, and P. Solinas, Destroying superconductivity in thin films with an electric field, Phys. Rev. Res. **4**, 033211 (2022).

[35] V. M. Fomin, *Self-rolled Micro- and Nanoarchitectures* (De Gruyter, Berlin, 2021).

[36] S. Chakraborty, D. Nikolić, J. C. Cuevas, F. Giazotto, A. Di Bernardo, E. Scheer, M. Cuoco, and W. Belzig, Microscopic theory of supercurrent suppression by gate-controlled surface depairing, Phys. Rev. B **108**, 184508 (2023).

[37] E. Piatti, D. Daghero, G. A. Ummarino, F. Laviano, J. R. Nair, R. Cristiano, A. Casaburi, C. Portesi, A. Sola, and R. S. Gonnelli, Control of bulk superconductivity in a BCS superconductor by surface charge doping via electrochemical gating, Phys. Rev. B **95**, 140501(R) (2017).

[38] L. D. Landau and E. M. Lifshitz, *Quantum Mechanics: Non-Relativistic Theory* (Butterworth-Heinemann, Oxford, 1981).

[39] L. N. Cooper, Bound electron pairs in a degenerate Fermi gas, Phys. Rev. **104**, 1189 (1956).

[40] V. F. Weisskopf, The formation of Cooper pairs and the nature of superconducting currents, Contemp. Phys. **22**, 375 (1981).

[41] J. Bardeen, L. N. Cooper, and J. R. Schrieffer, Theory of superconductivity, Phys. Rev. **108**, 1175 (1957).

[42] G. A. Ummarino and R. S. Gonnelli, Breakdown of Migdal's theorem and intensity of electron-phonon coupling in high-T_c superconductors, Phys. Rev. B **56**, R14279 (1997).

[43] J. P. Carbotte, Properties of boson-exchange superconductors, Rev. Mod. Phys. **62**, 1027 (1990).

[44] F. Marsiglio and J. P. Carbotte, Electron-phonon superconductivity, in *Superconductivity: Conventional and Unconventional Superconductors*, edited by K. H. Bennemann and J. B. Ketterson (Springer, Berlin, 2008), pp. 73–162.

[45] P. B. Allen and B. Mitrović, *Theory of Superconducting T_c*, Solid State Physics, edited by H. Ehrenreich, F. Seitz, and D. Turnbull (Academic Press, New York, 1983), Vol. 37, pp. 1–92.

[46] *Superconductivity, Vol. 1*, edited by R. D. Parks (Marcel Dekker, New York, 1969), p. 67.

[47] F. Marsiglio, Eliashberg theory of the critical temperature and isotope effect. dependence on bandwidth, band-filling, and direct Coulomb repulsion, J. Low Temp. Phys. **87**, 659 (1992).

[48] G. Ummarino, Eliashberg theory, in *Emergent Phenomena in Correlated Matter*, edited by E. Pavarini, E. Koch, and U. Schollwoeck (Forschungszentrum Jülich GmbH and Institute for Advanced Simulations, Jülich, 2013), pp. 13.1–13.36.

[49] E. R. Margine and F. Giustino, Anisotropic Migdal-Eliashberg theory using Wannier functions, Phys. Rev. B **87**, 024505 (2013).

[50] G. A. Ummarino and A. Zaccone, Quantitative Eliashberg theory of the superconductivity of thin films, J. Phys.: Condens. Matter **37**, 065703 (2025).

[51] E. Schachinger and J. P. Carbotte, Thermodynamic properties of strong coupling superconductors with energy-dependent electronic density of states, J. Phys. F **13**, 2615 (1983).

[52] W. E. Pickett, Effect of a varying density of states on superconductivity, Phys. Rev. B **21**, 3897 (1980).

[53] K. E. Kihlstrom, R. W. Simon, and S. A. Wolf, Tunneling $\alpha^2 f(\omega)$ from sputtered thin-film NbN, Phys. Rev. B **32**, 1843 (1985).

[54] Q. Zhang, H. Wang, X. Tang, W. Peng, and Z. Wang, Superconductivity dependence on epitaxial NbN film thickness, IEEE Trans. Appl. Supercond. **29**, 1 (2019).

[55] G. A. Ummarino, E. Piatti, D. Daghero, R. S. Gonnelli, I. Y. Sklyadneva, E. V. Chulkov, and R. Heid, Proximity Eliashberg theory of electrostatic field-effect doping in superconducting films, Phys. Rev. B **96**, 064509 (2017).

[56] A. Zaccone and V. M. Fomin, Theory of superconductivity in thin films under an external electric field, Phys. Rev. B **109**, 144520 (2024).

[57] E. J. Patiño and D. Lozano-Gómez, Quantum tunneling theory of Cooper pairs as bosonic particles, Sci. Rep. **11**, 9050 (2021).

[58] E. J. Nicol and J. P. Carbotte, Temperature dependence of the critical pair-breaking current in thin-film, strong-coupling superconductors, Phys. Rev. B **43**, 10210 (1991).

[59] P. G. de Gennes, *Superconductivity of Metals and Alloys* (CRC Press, Boca Raton, FL, 1999).

[60] M. Sidorova, A. Semenov, H.-W. Hübers, K. Ilin, M. Siegel, I. Charaev, M. Moshkova, N. Kaurova, G. N. Goltsman, X. Zhang, and A. Schilling, Electron energy relaxation in disordered superconducting NbN films, Phys. Rev. B **102**, 054501 (2020).

[61] J. R. Waldram, *Superconductivity of Metals and Cuprates* (CRC Press, Boca Raton, FL, 1996).

[62] M. Dressel and G. Grüner, *Electrodynamics of Solids: Optical Properties of Electrons in Matter* (Cambridge University Press, Cambridge, 2002).

[63] A. Y. Mironov, D. M. Silevitch, S. V. Postolova, M. V. Burdastyh, T. Proslier, T. I. Baturina, T. F. Rosenbaum, and V. M. Vinokur, Supercapacitance and superinductance of TiN and NbTiN films in the vicinity of superconductor-to-insulator transition, Sci. Rep. **11**, 16181 (2021).

[64] J. E. Hirsch, Electrodynamics of superconductors, Phys. Rev. B **69**, 214515 (2004).

[65] M. Tajmar, Electrodynamics in superconductors explained by proca equations, Phys. Lett. A **372**, 3289 (2008).

[66] L. Salasnich, Electrodynamics of superconductors: From Lorentz to Galilei at zero temperature, Entropy **26**, 69 (2024).

[67] M. C. Diamantini, S. V. Postolova, A. Y. Mironov, L. Gammaitoni, C. Strunk, C. A. Trugenberger, and V. M. Vinokur, Direct probe of the interior of an electric pion in a Cooper pair superinsulator, Commun. Phys. **3**, 142 (2020).

[68] M. L. Yu and J. E. Mercereau, Electric potentials near a superconducting-normal boundary, Phys. Rev. Lett. **28**, 1117 (1972).

[69] W. G. Jenks and L. R. Testardi, Electric-field penetration into superconducting and normal-state surfaces of $YBa_2Cu_3O_{7-x}$, Phys. Rev. B **48**, 12993 (1993).

[70] R. Tao, X. Xu, Y. Lan, and Y. Shiroyanagi, Electric-field induced low temperature superconducting granular balls, Physica C **377**, 357 (2002).

[71] P. Lipavský, J. Koláček, K. Morawetz, and E. H. Brandt, Electrostatic potential in a superconductor, Phys. Rev. B **65**, 144511 (2002).

[72] A. van Otterlo, M. Feigel'man, V. Geshkenbein, and G. Blatter, Vortex dynamics and the Hall anomaly: A microscopic analysis, Phys. Rev. Lett. **75**, 3736 (1995).

[73] J. Jackson, *Classical Electrodynamics*, 3rd ed. (Wiley, Hoboken, NJ, 1998).

[74] H. Y. Ku and F. G. Ullman, Capacitance of thin dielectric structures, J. Appl. Phys. **35**, 265 (1964).

[75] C. Black and J. Welser, Electric-field penetration into metals: consequences for high-dielectric-constant capacitors, IEEE Trans. Electron Devices **46**, 776 (1999).

[76] V. E. Kenner, R. E. Allen, and W. M. Saslow, Screening and tunneling at metal surfaces, Phys. Rev. B **8**, 576 (1973).

[77] A. Amoretti, Superconductors in strong electric fields: Quantum electrodynamics meets superconductivity, J. Phys.: Conf. Ser. **2531**, 012001 (2023).

[78] E. Piatti, D. Romanin, R. S. Gonnelli, and D. Daghero, Anomalous screening of an electrostatic field at the surface of niobium nitride, Appl. Surf. Sci. **461**, 17 (2018), 5th Progress in Applied Surface, Interface and Thin Film Science and Solar Renewable Energy News.

[79] D. van der Marel and C. Berthod, Superconductivity in metallic hydrogen, Newton **1**, 100002 (2025).

[80] R. Glover, III and M. Sherrill, Changes in superconducting critical temperature produced by electrostatic charging, Phys. Rev. Lett. **5**, 248 (1960).

[81] G. A. Ummarino, Strong-coupling behavior of the critical temperature of Pb/Ag, Pb/Cu and Pb/Al nanocomposites explained by proximity eliashberg theory, Condens. Matter **8**, 45 (2023).

[82] G. Ummarino, Superconductive critical temperature of Pb/Ag heterostructures, Physica C **568**, 1353566 (2020).

[83] G. A. Ummarino and D. Romanin, Theoretical explanation of electric field-induced superconductive critical temperature shifts in indium thin films, Phys. Status Solidi B **257**, 1900651 (2020).

[84] G. Ummarino and D. Romanin, Proximity two bands Eliashberg theory of electrostatic field-effect doping in a superconducting film of MgB_2, J. Phys.: Condens. Matter **31**, 024001 (2019).

[85] P. Allen, New method for solving Boltzmann's equation for electrons in metals, Phys. Rev. B **17**, 3725 (1978).

[86] G. Deutscher, H. Fenichel, M. Gershenson, E. Grünbaum, and Z. Ovadyahu, Transition to zero dimensionality in granular aluminum superconducting films, J. Low Temp. Phys. **10**, 231 (1973).

[87] M. Baggioli, C. Setty, and A. Zaccone, Effective theory of superconductivity in strongly coupled amorphous materials, Phys. Rev. B **101**, 214502 (2020).

[88] R. Travaglino and A. Zaccone, Extended analytical BCS theory of superconductivity in thin films, J. Appl. Phys. **133**, 033901 (2023).

[89] G. A. Ummarino and A. Zaccone, Can the noble metals (Au, Ag, and Cu) be superconductors? Phys. Rev. Mater. **8**, L101801 (2024).

[90] A. Deshpande, J. Pusskeiler, C. Prange, U. Rogge, M. Dressel, and M. Scheffler, Tuning the superconducting dome in granular aluminum thin films, J. Appl. Phys. **137**, 013902 (2025).

[91] K. Y. Arutyunov, E. A. Sedov, I. A. Golokolenov, V. V. Zav'yalov, G. Konstantinidis, A. Stavrinidis, G. Stavrinidis, I. Vasiliadis, T. Kekhagias, G. P. Dimitrakopulos, F. Komninu, M. D. Kroitoru, and A. A. Shanenko, Quantum size effect in superconducting aluminum films, Phys. Solid State **61**, 1559 (2019).

[92] D. López-Núñez, Q. P. Montserrat, G. Rius, E. Bertoldo, A. Torras-Coloma, M. Martínez, and P. Forn-Díaz, Magnetic penetration depth of aluminum thin films, arXiv:2311.14119.

[93] S. Qin, J. Kim, Q. Niu, and C.-K. Shih, Superconductivity at the two-dimensional limit, Science **324**, 1314 (2009).

[94] W. M. van Weerdenburg, A. Kamlapure, E. H. Fyhn, X. Huang, N. P. van Mullekom, M. Steinbrecher, P. Krogstrup, J. Linder, and A. A. Khajetoorians, Extreme enhancement of superconductivity in epitaxial aluminum near the monolayer limit, Sci. Adv. **9**, eadf5500 (2023).

[95] P. B. Allen and R. C. Dynes, Transition temperature of strong-coupled superconductors reanalyzed, Phys. Rev. B **12**, 905 (1975).